Research Article

Brief electrical nerve stimulation enhances intrinsic repair capacity of the focally demyelinated central nervous system

https://doi.org/10.4103/1673-5374.324848
Date of submission: December 22, 2020
Date of decision: January 19, 2021
Date of acceptance: April 30, 2021
Date of web publication: September 17, 2021

Lydia Ayanwuyi[1, 2], Nataliya Tokarska[1, 2, #], Nikki A. McLean[1, 2, #], Jayne M. Johnston[1, 2], Valerie M. K. Verge[1, 2, *]

Graphical Abstract *Increased neural activity enhances intrinsic repair of focally demyelinated axons in the central nervous system (CNS)*

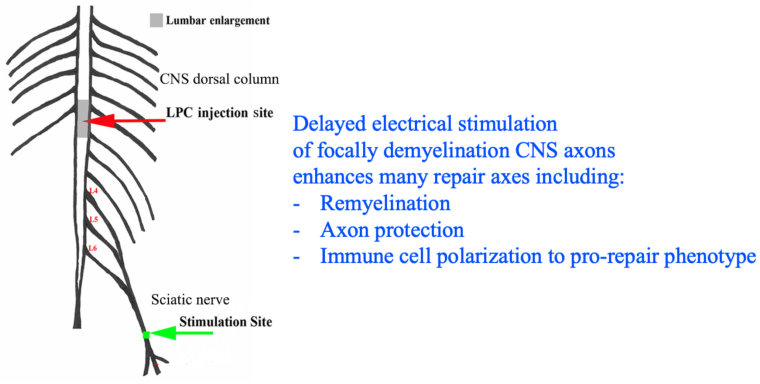

Abstract

Our lab has shown that brief electrical nerve stimulation (ES) has a dramatic impact on remyelination of lysophosphatidyl choline (LPC)-induced focally demyelinated rat peripheral nerves, while also inducing an axon-protective phenotype and shifting macrophages from a predominantly pro-inflammatory toward a pro-repair phenotype. Whether this same potential exists in the central nervous system is not known. Thus, for proof of principle studies, the peripheral nerve demyelination and ES model was adapted to the central nervous system, whereby a unilateral focal LPC-induced demyelination of the dorsal column at the lumbar enlargement where the sciatic nerve afferents enter was created, so that subsequent ipsilateral sciatic nerve ES results in increased neural activity in the demyelinated axons. Data reveal a robust focal demyelination at 7 days post-LPC injection. Delivery of 1-hour ES at 7 days post-LPC polarizes macrophages/microglia toward a pro-repair phenotype when examined at 14 days post-LPC; results in smaller LPC-associated regions of inflammation compared to non-stimulated controls; results in significantly more cells of the oligodendroglial lineage in the demyelinated region; elevates myelin basic protein levels; and shifts the paranodal protein Caspr along demyelinated axons to a more restricted distribution, consistent with reformation of the paranodes of the nodes of Ranvier. ES also significantly enhanced levels of phosphorylated neurofilaments detected in the zones of demyelination, which has been shown to confer axon protection. Collectively these findings support that strategies that increase neural activity, such as brief electrical stimulation, can be beneficial for promoting intrinsic repair following focal demyelinating insults in demyelinating diseases such as multiple sclerosis. All animal procedures performed were approved by the University of Saskatchewan's Animal Research Ethics Board (protocol# 20090087; last approval date: November 5, 2020).

Key Words: axon protection; demyelination; immune response; lysophosphatidyl choline; macrophage; microglia; multiple sclerosis; myelin; nervous system repair; neural activity; polarization

Chinese Library Classification No. R459.9; R364; R741

Introduction

Multiple sclerosis (MS) is a central nervous system (CNS) inflammatory disease characterized by immune-mediated segmental demyelination and variable degrees of axonal and neuronal degeneration. Efficient repair of demyelinated lesions is a major challenge of MS. Conventional therapies largely focus on modulation of the immune response responsible for lesion generation (Clerico et al., 2008; Nakahara et al., 2009). While alleviating some symptoms and damage, it does not adequately tackle the task of remyelinating damaged areas

[1]Department of Anatomy, Physiology and Pharmacology, University of Saskatchewan, Saskatoon, SK, Canada; [2]Cameco MS Neuroscience Research Center, University of Saskatchewan, Saskatoon, SK, Canada
***Correspondence to:** Valerie M. K. Verge, PhD, valerie.verge@usask.ca.
https://orcid.org/0000-0001-6648-3242 (Valerie M. K. Verge)
#These authors contributed equally to the work.

Funding: *This work was supported by Multiple Sclerosis Society of Canada (MSSOC), No. 2362 (to VMKV); Canadian Institutes of Health Research (CIHR), No. 14238 (to VMKV). LA and NT were supported by University of Saskatchewan College of Medicine Research Awards (CoMGRADs).*
How to cite this article: *Ayanwuyi L, Tokarska N, McLean NA, Johnston JM, Verge VMK (2022) Brief electrical nerve stimulation enhances intrinsic repair capacity of the focally demyelinated central nervous system. Neural Regen Res 17(5):1042-1050.*

or preventing axon degeneration which increase disability associated with progressive forms of MS (Mahad et al., 2015; Singh et al., 2017; Faissner et al., 2019). As only a small fraction of MS patients will see significant remyelination (Prineas and Connell, 1979; Nakahara et al., 2009), strategies to augment repair and gain further insight into what drives myelin plasticity (Monje 2018) are needed.

Therapies such as brief electrical nerve stimulation (ES) enhance the intrinsic repair mechanisms of the injured peripheral nervous system, including remyelination (Al-Majed et al., 2000a, b; Geremia et al., 2007; Gordon et al., 2009). With respect to demyelinating pathologies, ES has a dramatic impact on remyelination of lysophosphatidyl choline (LPC)-induced focally demyelinated peripheral nerves, while also improving other repair indices (McLean et al., 2014; McLean and Verge, 2016). These include increased myelin basic protein (MBP) expression and node of Ranvier re-organization in a pattern consistent with remyelination, increased levels of brain derived neurotrophic factor (BDNF), a pro-myelinating molecule (McTigue et al., 1998; Zhang et al., 2000; Chan et al., 2004; Fletcher et al., 2018), increased levels of phosphorylated neurofilaments (pNF) that help protect the axon (Goldstein et al., 1987; Pant, 1988; Greenwood et al., 1993; Pant and Veeranna, 1995), increased clearance of macrophages and myelin debris critical for remyelination (Kotter et al., 2005, 2006; Neumann et al., 2009), and attenuation of reactive gliosis.

While important advances in understanding the role of axonal activity and the axo-glial communication in the myelination process have been made (Ishibashi et al., 2006; Kukley et al., 2007; Wake et al., 2011), we still have little insight about the therapeutic potential that increasing neural activity has on CNS repair indices *in vivo* beyond that described for myelination (Kukley et al., 2007; Gibson et al., 2014; Mitew et al., 2018). Given the promising impacts ES has in the peripheral nerve focal demyelination model, we have adapted it to the CNS. We created a reproducible discrete unilateral focal dorsal column (DC) demyelination at the lumbar enlargement just above where sciatic nerve afferents enter, so that subsequent sciatic nerve ES would result in increased neural activity in this region. Examination of the impact ES on repair following focal DC demyelination revealed significant impacts on multiple repair indices. These include increased expression of an axon-protective phenotype, enhanced presence/recruitment of cells in the oligodendroglial lineage to the site of demyelination, increased levels of myelin basic protein observed in linearized structures, increased presence of Caspr positive paranodal structures in the demyelination zones and polarization of activated macrophages/microglia in these zones toward a pro-repair phenotype.

Materials and Methods

Animals and reagents

All animal procedures performed were approved by the University of Saskatchewan's Animal Research Ethics Board (protocol#20090087; last approval date: November 5, 2020) and adhered to Canadian Council on Animal Care guidelines for humane animal use. Animals were given buprenorphine (0.05–0.1 mg/kg) subcutaneously pre- and postoperatively to alleviate incisional pain. A total of 32 young adult male Wistar rats (age 7 weeks, body weight 150–200 g) were used in the study. All animals were acclimated for 7 days before handling or any procedures. Animals were housed in groups of 2 per cage except for post-surgery where they were singly housed for 4 days to allow for post-operative observation. The Animal Care Facility maintained a controlled environment with a temperature of 20 ± 1°C and an alternating 12-hour light/dark schedule.

Unless otherwise stated all chemical used were obtained from Sigma-Aldrich Canada (Oakville, ON, Canada).

DC unilateral focal demyelination and ES

Under deep anesthesia with inhaled isoflurane (2% delivered at a rate of 2 L/min; Fresenius Kabi, Toronto, ON, Canada), animals were placed in a stereotaxic apparatus (David Kopf Instruments, Tujunga, CA, USA) and the lumbar dorsal columns of adult male Wistar rats were exposed by a laminectomy at the level where the sciatic nerve afferents enter. The spinal cord was then stabilized using the spinal stabilization vertebral clamp. The dorsal column was unilaterally focally demyelinated at ~T12 via a 2 µL injection of 1% lyso-phosphatidyl choline (LPC) with 0.7% Fluorogold (FG; Fluorochrome Inc. Denver, CO, USA; **Figure 1**) in sterile saline into the right DC at a depth of 1 mm using a Hamilton Neurosyringe with a 33-gauge needle (Fisher Scientific Canada, Ottawa, ON, Canada) at a rate of 0.1 µL per minute. The needle is left in place for 5 minutes post-injection to ensure diffusion into the spinal cord. The laminectomy area was covered with a small piece of sterile gelfoam (Pfizer Canada, North York, ON, Canada). Seven days later, the animals were randomly assigned to treatment groups (n = 8 and 16 for 7- and 14-day LPC, respectively). Four naïve rats served as controls.

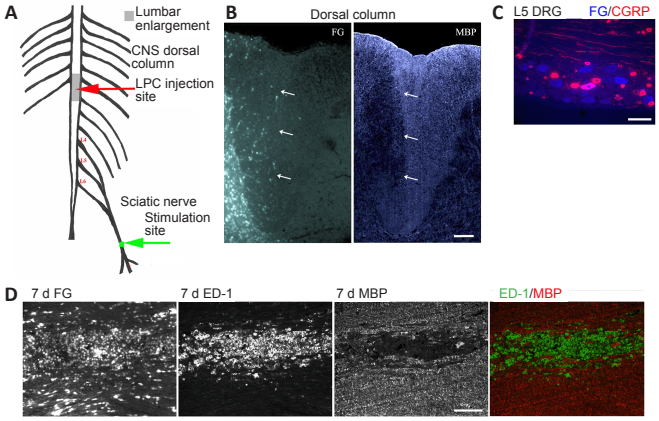

Figure 1 | Experimental model - unilateral myelin loss localizes to FG-postive regions 7 days post LPC-induced demyelination of the right dorsal columns.

(A) CNS focal demyelination model +/- delayed electrical stimulation (ES)- at 7 days post-LPC. (B) Transverse right dorsal column section 7 days post LPC/FG injection showing paucity of MBP immunofluorescence (IF) in FG-postive region (arrows). (C) L5 DRG section showing retrograde transport of FG (blue) by L5 sensory afferents. Thereby assuring correct level of the dorsal columns was affected by sciatic nerve electrical stimulation. Note that only large size neurons appear to be FG-postive and only a single large calcitonin gene-related peptide (CGRP) IF-postive neuron (pink) is dual labelled, as would be expected for myelinated axons within the dorsal columns affected by the LPC/FG injection. (D) Longitudinal section of 7 day LPC-focally demyelinated right dorsal columns processed for dual ED-1 and MBP IF reveals loss of myelin (MBP) area coincides with FG intense area and region of activated macrophages/microglia as detected by the ED-1/MBP IF. Merged images of the ED-1 (green) and MBP (red) IF (below) demonstrate the localization of activated macrophages/microglia to regions of myelin loss. Scale bars: 100 µm for B–D. FG: Fluorogold; LPC: lysophosphatidyl choline; MBP: myelin basic protein.

The 8 rats in the 7-day LPC group were used to visualize and characterize the lesion induced prior to treatment, while an additional 4 rats that had been injected with vehicle alone 7 days prior served as LPC injection controls.

In the 14-day LPC lesion group 6 rats were deeply anesthetized and the sciatic nerve on same side as the LPC injection exposed at mid-thigh 7 days post-LPC injection and subjected to 1-hour continuous 20 Hz ES. To do so, stainless steel wires were bared of insulation (2–3 mm for the anode, 5–10 mm

for the cathode) and connected to a Grass SD-9 Stimulator (Quincy, MA, USA). The cathode wire was wrapped around the exposed nerve, 2–3 mm proximal to sciatic nerve trifurcation site. The anode was placed between the skin and muscle. ES was performed as described (Al-Majed et al., 2000b) delivering a continuous 20 Hz train of supramaximal pulses (100 ms, 3 V) for 1 hour, parameters that closely mimic firing patterns of motor and sensory neurons (Fitzgerald, 1987; Al-Majed et al., 2000b). These rats were left an additional 7 days to examine the impact of ES on the repair processes induced by ES. To generate controls for the ES, 4 additional animals injected with LPC 7 days previous were deeply anesthetized and had the sciatic nerve on same side as the LPC injection exposed at mid-thigh. A 2% lidocaine soaked gelfoam was applied to the sciatic nerve proximal to ES 30 minutes prior to and during the ES procedure (n = 4) followed by a thorough rinse with sterile PBS before closure of the incision in layers. These rats were also left an additional 7 days to examine the impact of blocking nerve stimulation on repair responses. The remaining 6 rats in the 14-day LPC group received no treatment.

At the end of the designated periods, the animals were perfused via the aorta with 4% paraformaldehyde and the spinal cord lumbar enlargement (surrounding the lesion site) and L4,5 DRG tissues removed, post-fixed, cryoprotected in 20% sucrose, embedded in cryomolds with OCT compound (Tissue Tek, Fisher Scientific Canada) and frozen in cooled isopentane. To ensure processing under identical conditions, tissue from experimental and control animals were placed in the same cryomold, sectioned and kept at –80°C prior to processing for immunohistochemical analyses.

Immunofluorescence histochemistry

Transverse or longitudinal lumbar spinal cord sections that included the demyelinated lesion (as verified by presence of FG immunofluorescence) were cut at a thickness of 10 µm on a cryostat with control (Naïve; LPC) and experimental (LPC + ES) tissue mounted on the same slide. Slides were air-dried for 15 minutes and washed in PBS prior to blocking in Sea Block Buffer (Cat# ab166951; Abcam, Cambridge, MA, USA) for 1 hour at room temperature, then incubated overnight at 4°C with primary antibodies diluted in 10% Sea Block and 0.1% Triton X-100 in PBS. With the exception of the Olig2 antibody, all antibodies employed in this study were validated by Western blot in our previous studies examining the impact of ES on repair of focally demyelinated regions of peripheral nerve (Mclean et al., 2014; McLean and Verge, 2016). Antibodies used in the present study include mouse anti-MBP (Cat# 808402, dilution 1:250; BioLegend, San Diego, CA, USA), rabbit anti-Olig2 (Cat# AB9610, dilution 1:1000; EMD Millipore, Oakville, ON, Canada), rabbit anti-Contactin-associated protein 1 (Caspr; Cat# ab3415, dilution 1:4500, Abcam), and mouse anti-SMI-31 (phosphorylated neurofilament, Cat # SMI-31R, dilution 1:1000, Biolegend), mouse anti-ED1 (CD68; Cat# MCA341R, dilution 1:250; Bio-Rad, Mississauga, ON, Canada), mouse anti-beta III tubulin (βIII-tubulin; Cat# MAB1637, dilution 1:100, EMD Millipore), rabbit anti-TNF-α 1:100 (Cat# ab6671, dilution 1:100, Abcam), rabbit anti-Arginase 1 (Arg1; Cat# sc20150, dilution 1:100; Santa Cruz Biotech, Dallas, TX, USA) and mouse anti-calcitonin gene-related peptide (CGRP; Cat# ab81887, dilution 1:100, Abcam). Slides were washed in PBS and fluorophore-coupled secondary antibodies (Alexa Fluor 488 conjugated donkey anti-mouse (dilution 1:1000, Jackson ImmunoResearch, West Grove, PA, USA) and Cy3-conjugated donkey anti-rabbit (dilution 1:1000, Jackson ImmunoResearch) were applied for one hour at room temperature. Slides were washed in PBS and mounted with a coverslip using Fluoroshield (Cat# ab104139, Abcam). Tissue sections were visualized using a Zeiss Axio Imager M.1 microscope (Zeiss Canada, North York, ON, Canada) at 20× and 40× magnification. The demyelinated area was identified by the presence of FG-positive staining and verification of the level of demyelination verified by the presence of FG retrogradely transported from the injection region in corresponding L4,5 DRG sections (**Figure 1**). Images were digitally captured under identical conditions using Northern Eclipse v7.0 software (EMPIX Imaging Inc., Mississauga, ON, Canada).

Data analysis

Four separate biological/experimental runs with a minimum of 2 rats in each LPC+/-ES experimental group were conducted and tissue processed for immunofluorescence to generate the slides assessed in this study. Localization of the FG fluorescence to the DC ipsilateral to lesion, combined with perturbations in MBP expression in this region and the presence of FG in corresponding ipsilateral but not contralateral L4,5 DRG neurons (**Figure 1**) were used as inclusion criteria for the analysis. This indicated that the injection was in the area of the DC which includes the sciatic nerve afferents and that it had been unilaterally focally demyelinated, and that these axons would be stimulated when the sciatic nerve was subjected to the brief ES at 7 days post-LPC. To ensure accurate analysis of relative changes in immunofluorescence (IF) signal between experimental groups, spinal cord segments containing LPC injection from both experimental (LPC + ES) and control groups (LPC only, Naïve, and Naïve + saline) were always mounted on the same slide so that processing was conducted under identical conditions. Within these groupings, the best four animals/experimental group with lesions localized to the dorsal column ipsilateral to the stimulated nerve were selected for detailed quantitative analysis, with 8–16 fields of interest photographed and analyzed per experimental condition per marker.

Immunofluorescence data was gathered from digital images of naïve tissue or from the site of demyelination captured under identical exposure conditions using Northern Eclipse v7.0 software (EMPIX Imaging Inc.) and a Zeiss Axio Imager M.1 fluorescence microscope (Zeiss Canada). Demyelinated regions of interest (ROIs) were identified by the presence of intense FG-positive staining combined with ED-1 immunofluorescence. Analysis was carried out by tracing the outline of the FG/ED1-positive regions of interest using Northern Eclipse and then either calculating (i) the Average Gray/unit area within the ROI for the marker in question (TNF-α; Arg1); (ii) determining the density of Olig2-positive cells by counting the number of these cells within measured DC demyelinated regions of interest to obtain density measurements/mm^2; (iii) the percentage of the focally demyelinated ROI occupied by the phosphorylated form of neurofilament (as detected by the SMI-31 antibody) was determined by thresholding the SMI-31 positive profiles, then assessing what percentage of the area of interest occupied by the thresholded SMI-31-positive profiles; or (iv) in the case of detectable Caspr-positive paranodes, the density of these within either naive or focally demyelinated experimental DC regions was assessed by first defining the ROI by looking for a combination of MBP perturbations and intense FG presence, measuring this area and then counting all Caspr-positive paranodes in the circumscribed area. Eight to 16 fields of interest/marker/experimental condition were captured and analyzed as described above, in a manner blinded to experimental condition.

Statistical analysis

Statistical analysis was performed using one-way analysis of variance (ANOVA) with Bonferroni's *post hoc* test analysis (Graph Pad Prism v5.0; GraphPad Software, San Diego, CA, USA). Results achieved statistical significance at a P-value < 0.05.

Results

Focal demyelinating lesion model

In order to examine the impact of increased neural activity on the many aspects of repair following a focal CNS demyelinating lesion, we developed a model that generates reproducible lesions. We employed a stereotaxic DC focal demyelination model where a unilateral DC demyelinating lesion was created just slightly above the level of spinal cord where the sciatic nerve afferents enter, by co-injecting LPC with the retrograde tracer FG. The FG is vital for defining regions initially affected, especially when examining later timepoints, when repair can be advanced. To make the model more clinically relevant, brief 1-hour electrical stimulation (ES; 20 Hz) of the sciatic nerve ipsilateral to the focal demyelinating lesion was only performed one week after the LPC/FG lesion was induced. This allows assessment of ES treatment on intrinsic cellular repair and remyelination responses (**Figure 1A** and **B**).

Examination of the lesions at 7 days post-LPC revealed an excellent register between the lack of MBP, an elevated immune response, as characterized by the presence of activated macrophages/microglia (ED-1 positive cells) and the intense FG staining (**Figure 1D**), as observed in our PNS demyelinating model (McLean et al., 2014). At all experimental timepoints examined, L4,5 dorsal root ganglia (DRG) were removed to examine whether FG was also detectable in the L4,5 DRG neurons ipsilateral to injection. This provides further evidence that the focal demyelinated region included the sciatic nerve afferents (**Figure 1C**) and thus the ES would affect these axons in the demyelination zone. We also co-localized the retrogradely labelled DRG with calcitonin gene-related peptide IF, as this marker labels the NGF-responsive nociceptive subpopulation of sensory neurons that are predominantly small to medium size unmyelinated c-fibres (Verge et al., 1989). The unmyelinated c-fibres which are confined to the gray matter of the dorsal horn should not be labelled with FG when the injection is done properly and remains confined to the DCs. Only the few large size thinly myelinated CGRP-positive neurons contribute axons to the DCs (Tamatani et al., 1989). As seen in **Figure 1C**, many large size neurons are FG-positive, but only one is co-labelled with CGRP IF, while none of the small to medium size CGRP positive neurons contained FG. It was also noted that in all animals where intense FG staining was observed in the dorsal column 7 days post-LPC injection, there was an associated focal demyelination lesion lacking linear MBP staining (**Figure 1D** and **E**).

LPC injection controls included a group of animals where sterile saline (vehicle control) was injected in place of the LPC/FG. In this control group, no discernible loss of myelin basic protein was observed and only a minimal injection-related immune response could be seen, with a few ED-1-positive cells detected along the needle injection site (data not shown). Controls for the ES group included focally demyelinated tissue with lesions of the same duration but no stimulation and a group of animals where the impact of 1-hour ES delivered at 7 days post-LPC injection was blocked by the application of lidocaine prior and during the electrical stimulation period according to previous reports (McLean et al., 2014; McLean and Verge, 2016). Similar to the findings in the McLean studies, outcomes in the lidocaine-treated animals were not discernibly different from the animals which received only the focal LPC demyelinating lesion (data not shown). Thus, the impact of ES on the parameters examined in this study was likely due to neuronal activation, because they were abolished when lidocaine was applied. We next examined the impact of the brief 1-hour ES administered 7 days post-LPC injection on repair and axon protective indices. This time point was selected as it allows examination of the impact of the therapeutic intervention at a timepoint when robust demyelination has occurred and thus in need of repair. Further, the examination of outcomes 1 week later, namely 14 days post-LPC injection and 1 week post ES, was selected as it allows for assertation of whether the brief 1-hour ES improves repair at a timepoint where there is normally still only robust demyelination and is two weeks prior to the timepoint by which spontaneous remyelination will have occurred in this model (Jeffery & Blakemore, 1995; Kateria et al., 2017).

Impact of ES on expression of phosphorylated neurofilament expression in zones of focal demyelination

A previous work (McLean et al., 2014) has shown that focal demyelination of the tibial nerve results in a loss of phosphorylated neurofilament expression as detected by the absence of SMI-31 IF, despite the fact that the axons are still detectable and express βIII-tubulin. Notably, in that study, brief 1-hour ES resulted in a rapid re-expression of phosphorylated neurofilaments in the demyelination zone, that coincided with elevated BDNF expression (McLean et al., 2014), a molecule previously shown to effect neurofilament phosphorylation (Tokuoka et al., 2000).

In longitudinal sections of naïve DC processed for dual MBP/SMI-31 IF, we observed that abundant linear MBP immunoreactivity was associated with linear axonal structures expressing phosphorylated neurofilaments as detected by the antibody SMI-31 (**Figure 2A**). This is in contrast to the greatly reduced levels observed 7 days following LPC/FG injection that also resulted in a loss of linear MBP immunoreactivity in the focally demyelinated region identified by the intense FG staining (**Figure 2B**). One week later (**Figure 2C** – 14 days), there is still greatly reduced levels of phosphorylated neurofilament expression in the FG-intense demyelinated region, with many round punctate MBP-positive profiles suggesting there is still much myelin debris in the zone 14 days post injection of LPC. The punctate MBP-positive profiles are consistent with the morphology of ED-1 positive cells that we observe filled with myelin debris in this experimental group (data not shown). Brief 1-hour ES delivered at 7 days post-LPC resulted in significantly increased levels of linear SMI-31 positive staining in the focally demyelinated zone with intense FG staining, supporting that the increased neural activity conferred an axon-protective phenotype. The increased expression of phosphorylated neurofilaments was coupled with increased linear MBP-positive profiles in the FG intense region and reduced evidence of myelin debris (**Figure 2D** – 14 days + ES). Merged images from the FG-intense demyelinated zone revealing a good register of MBP and SMI31 staining (**Figure 2E**), supporting that these axons have likely been remyelinated.

Quantification of the percentage of the focally demyelinated area (delineated by intense FG staining) occupied by phosphorylated neurofilaments revealed that ES resulted in significantly increased levels of phosphorylated neurofilaments in the FG-intense demyelination zone (**Figure 2F**).

Impact of ES on density of oligodendroglial-lineage cells localized to regions of focal demyelination

We next examined whether the increased levels of linear MBP structures observed in zones of demyelination in response to ES were associated with an increased presence of cells of the oligodendroglial lineage [oligodendrocyte precursor cells (OPCs) and oligodendrocytes]. This was done by assessing the density of cells with nuclear Olig-2 in the regions of focal demyelination, a transcription factor identifying OPCs and oligodendrocytes in the oligodendroglial lineage (Valério-Gomes et al., 2018).

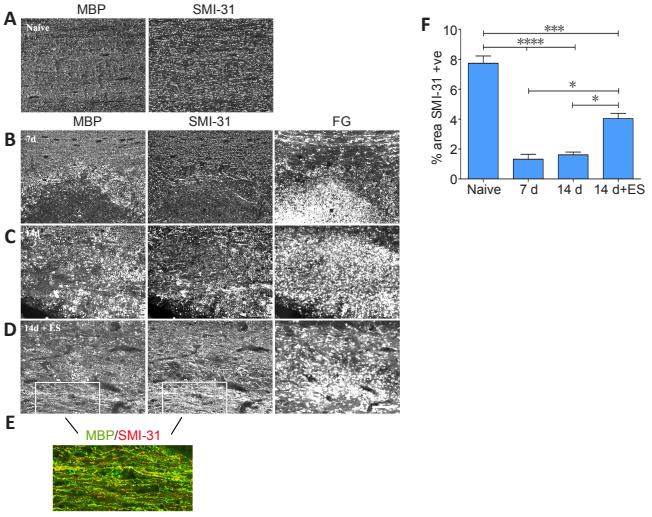

Figure 2 | ES promotes an axon protective phenotype in focally demyelinated regions of DC.

(A) Longitudinal dorsal spinal sections of dorsal columns (DC) from a naïve animal dually processed for MBP and phosphorylated neurofilament (pNFM/ SMI-31) immunofluorescence (IF). (B–E) Fluorogold (FG)-positive focally demyelinated DC areas on longitudinal dorsal spinal sections dually processed for MBP and phosphorylated neurofilament (pNFM/ SMI-31) IF at time points post-LPC injection as indicated. At 7 days post-LPC (B) focally demyelinated regions are largely devoid of pNFM. One hour ES at 7 days post-LPC significantly promotes expression of pNFM in regions that are also undergoing increased myelination (14 days + ES; D) relative to non-stimulated controls at 14 days post-LPC (C). Note: the non-stimulated 14 days focally demyelinated region appears to be still actively clearing myelin debris as denoted by the presence of many MBP-positive round cells consistent with macrophage/ microglia morphology and lack linear SMI-31 positive structures in the FG-intense/focally demyelinated region, as opposed to the presence of many more linear MBP and SMI-31 structures in the ES treated tissue. (E) Enlarged merged picture of boxed regions in D of a section processed for dual MBP (green) and SMI-31 (red) IF showing a high degree of colocalization of myelin over axons with phosphorylated neurofilaments in FG rich regions, supportive of remyelination of SMI-31 positive axons. Scale bars: 100 µm for A–D and 50 µm for E. (F) Quantification of % of region occupied by pNFM/SMI-31-positive (+ve) axons in dorsal columns of naïve or focally demyelinated regions defined by corresponding intensely FG-positive areas. Data are expressed as the mean ± SEM. $n = 4$ animals analyzed/experimental group. $^{*}P < 0.05$, $^{***}P < 0.001$, $^{****}P < 0.0001$ (one-way analysis of variance with Bonferroni's *post hoc* analysis).

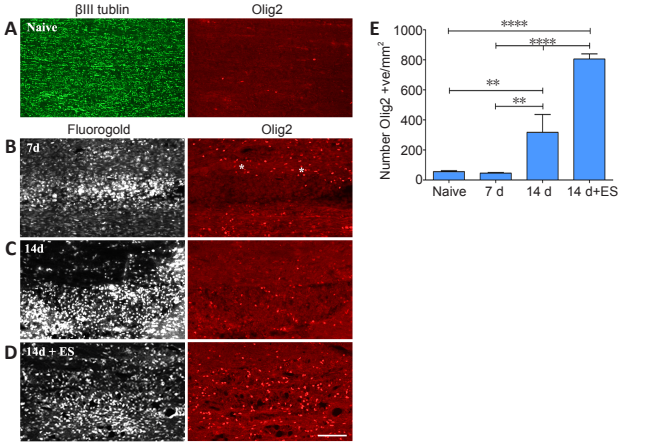

Figure 3 | ES promotes recruitment of cells of the oligodendroglial lineage to regions of focal demyelination.

(A) Few Olig2-positive cells are detected in longitudinal sections of lumbar DCs processed for dual immunofluorescence to detect Olig2 and the axon marker βIII-tubulin. (B–D) Photomicrographs from FG-intense focally demyelinated DC regions (left column) on longitudinal dorsal spinal cord sections processed for Olig2 (right column) immunofluorescence (IF). FG intense areas which coincide with focally demyelinated DC regions reveal a paucity of Olig2- positive (red cells) in these areas 7 days (B) post-LPC injection. (C) By 14 d post-LPC more Olig2 positive cells are evident in the the demyelinated zone. Note that Olig2-positive cells surround the 7 days focally demyelinated region (asterisks) while ES results in significantly more Olig2 positive cells in the focally demyelinated region by 14 days post-LPC (14 d + ES; D). Scale bar: 100 µm for A–D. (E) Quantification of the density of Olig2 positive (+ve) cells present in naïve dorsal columns or in focally demyelinated regions +/– ES (defined by corresponding intense FG positive areas) reveals that ES significantly increases their density in the demyelinated zone. Data are expressed as the mean ± SEM. $n = 4$ animals analyzed/experimental group. $^{**}P < 0.01$, $^{****}P < 0.0001$ (one-way analysis of variance with Bonferroni's post hoc analysis). DC: dorsal column; ES: electrical stimulation; FG: Fluorogold.

In naïve DCs, where linear axonal profiles are identified by βIII-tubulin IF, very few Olig-2 positive cells are present (**Figure 3A**). By 7 days following the focal demyelinating lesion, few Olig2-positive cells are observed in the focally demyelinated FG intense regions, although many can be seen in the regions bordering the lesion (**Figure 3B** and **E** – 7 days), consistent with the migration of cells of the oligodendroglial lineage to the demyelination zone without infiltration (Boyd et al., 2013). However, by 14 days post-LPC, significantly more Olig2-positive cells are observed in the zone of focal demyelination with a highly significant increase in density in this zone in response to ES (**Figure 3C–E** – 14 days; 14 days + ES).

Impact of ES on number of paranodal regions detected in demyelination zones

The increased presence of linear MBP-positive profiles observed in the demyelination zone in the stimulated animal is suggestive of increased myelination. To provide additional proof that this had occurred, we examined a structural marker of the paranodal region of the nodes of Ranvier. The paranodal protein Caspr was selected as a marker of paranodal regions as it is critical for nodal stability, tethering it to the axonal membrane, preventing diffusion of ion channels away from the node, a region that forms upon successful myelination (Suminaite et al., 2019).

In naive DCs, MBP expression is accompanied by abundant Caspr-positive aggregates/paranodal regions (**Figure 4A** and **F** – Naïve). However, 7 days following a focal demyelinating lesion, these nodal regions are largely undetectable with only a few visible on the boundaries of the demyelination zone (**Figure 4B** and **F** – 7 days). At 14 days post-LPC injection, the reappearance of a few linear MBP-positive structures can be observed and associated with these are a few Caspr-positive profile/aggregates, consistent with the paranodal regions of nodes of Ranvier (**Figure 4C** and **F** – 14 days). ES resulted in the reappearance of many more linear MBP structures in the demyelination zone with significantly more Caspr-positive paranodal regions detected, reaching about a third of the density observed in naïve DCs (**Figure 4D** and **F** – 14 days + ES) and these are associated with the linear MBP-positive profiles (**Figure 4E** – 14 days + ES). These observations combined with the increased MBP positive linear profiles in the stimulated DCs, support that more effective remyelination appears to have taken place in response to the 1-hour ES treatment.

Impact of ES on polarization of activated macrophages/ microglia toward a pro-repair state in focally demyelinated DC

The role of peripherally-derived macrophages and their CNS counterpart, microglia, in repair of the central nervous system is highly debated, especially in MS where macrophages/ microglia are implicated in both demyelination and remyelination disease phases (David and Kroner, 2011; Rawji and Yong, 2013; Miron and Franklin, 2014). While microglia and macrophages contribute to autoimmune disease through the release of toxins and via antigen presentation to cytotoxic lymphocytes (Banati et al., 1993; Myers et al., 1993; Cash et al., 1994), they are also beneficial, phagocytosing myelin debris and secreting growth factors. They exist in a continuum of activation states making them highly dynamic cells, polarizing into pro-inflammatory "classically activated" M1

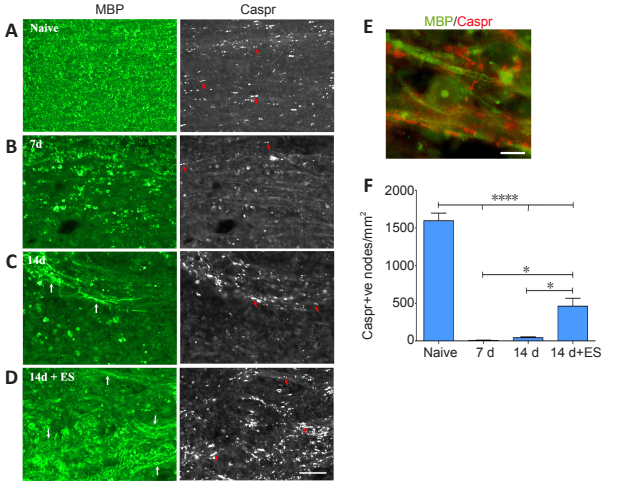

Figure 4 | ES promotes reappearance of Caspr-positive paranodal regions in 14 day focally demyelinated dorsal columns.

Longitudinal sections of spinal cord dorsal columns (DC) show a positive correlation between abundant myelin staining (MBP; green) in DC and number of punctate aggregates of paranodal protein Caspr on either side of the node (examples-red arrows). All post-LPC timepoint pictures are taken from FG intense regions coinciding with the focally demyelinated regions. Seven days following focal demyelination (B), myelin is lost with MBP localizing to round cells consistent with macrophage morphology. Caspr-positive paranodes (red arrows) are only detected along the boundaries of the focally demyelinated area. By 14 days post-LPC (14 days; C) a few nodes are detected (examples-red arrows) in regions appearing to undergo remyelination (white arrows). ES (14 days + ES; D) increases the numbers of Caspr-positive paranodes in the demyelinated regions (examples-red arrows) which have increased MBP (white arrows) consistent with enhanced remyelination. (E) High power example of Caspr-positive paranodal regions (red) associated with linear MBP (green) within previously demyelinated zone in 14 days + ES animal. Note the appearance of a MBP-positive circular cell, likely a macrophage/microglia that has phagocytosed myelin. Scale bars: 50 µm for A–D and 10 µm for E. (F) Quantification of the number of Caspr-positive (+ve) paranodes detected/mm2 of focally demyelinated DC regions reveals a significant increase in the density of paranodes detected in response to ES relative to focal demyelination alone. Data are expressed as the mean ± SEM. $n = 4$ animals analysed/experimental group. *$P < 0.05$, ****$P < 0.0001$ (one-way analysis of variance with Bonferroni's *post hoc* analysis).

macrophages with the "alternatively activated" pro-repair M2 phenotype representing the opposite end of the spectrum. Thus, to gain insight into whether ES treatment might be polarizing activated macrophages/microglia toward a pro-repair state we examined the impact of brief ES on levels of expression of the pro-repair molecule Arg-1 versus the pro-inflammatory molecule TNF-α longitudinal sections of DCs that include the focal demyelination zone were processed for dual immunofluorescence to detect the presence either Arg-1 (**Figure 5**) or TNF-α (**Figure 6**) in regions occupied by activated macrophages/microglia expressing ED-1, which also coincide with the FG intense regions (not shown). Naïve tissue was not assessed due to the absence of activated macrophages/microglia in this state. At 7 days post-LPC, the ED-1 positive macrophages/microglia displayed high levels of TNF-α IF (**Figure 6A** and **E**) relative to the low levels of Arg-1 IF (**Figure 5A** and **E**) observed in these cells, properties that remained relatively unchanged for Arg-1 one week later (14 days; **Figure 5B** and **E**), but were significantly reduced for TNF-α (14 days; **Figure 6B** and **E** – 14 days). Brief ES resulted in a qualitative reduction in numbers of activated macrophages/microglia detected; ES also polarized the remaining macrophages/microglia toward a pro-repair phenotype with significantly increased levels of Arg-1 (**Figure 5C–E** – 14 days + ES) and significantly decreased levels of TNF-α (**Figure 6C–E** – 14 days + ES). The smaller ED-1-positive region would also suggest that ES drives a faster resolution of the immune response. Finally, both Arg-1 and TNF-α immunoreactivity was observed in cells and structures other than ED-1-positive activated macrophages/microglia (**Figures 5** and **6**), consistent with previous reports of expression in astrocytes and neurons in addition to macrophages/microglia (Chung and Benveniste 1990; Breder et al., 1993; Gahring et al., 1996; Ahn et al., 2012; Choi et al., 2012; Quirié et al., 2013).

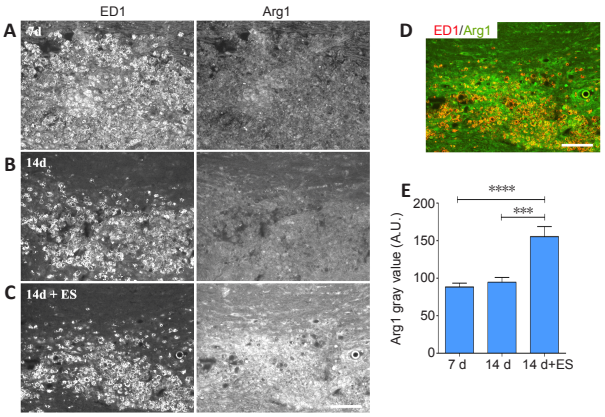

Figure 5 | Delayed brief ES increases levels of pro-repair molecule Arginase-1 (Arg1) in activated macrophages/microglia (ED-1) localizing to regions of focal DC demyelination.

(A–C) Longitudinal sections of dorsal spinal cord processed for dual immunofluorescence to detect activated microglia/macrophages (ED-1) and Arg1. Prominent infiltration of low Arg1 expressing ED-1-positive macrophages/microglia cells into the demyelination zone occurs 7 days post-LPC/FG injection (A). One-hour ES at 7 days post-LPC increases the level of Arg1 detected in macrophages/microglia at 14 days (14 days + ES; C) relative to levels in inflamed regions 14 days post-LPC. (B) Note: the immune response (ED-1 intense regions appears to be more resolved in 14 days + ES tissue. (D) merged ED-1 (red) and Arg1 (green) images from (C) show a high level of Arg1 expression (orange) in the remaining macrophages/microglia in response to ES. Scale bar: 100 µm for A–D. (E) Quantification of alterations in immunofluorescence signal intensity in focally demyelinated regions confirms qualitative observations. Data are expressed as the mean ± SEM. $n = 4$ animals analysed/experimental group. ***$P < 0.001$, ****$P < 0.0001$ (one-way analysis of variance with Bonferroni's *post hoc* analysis).

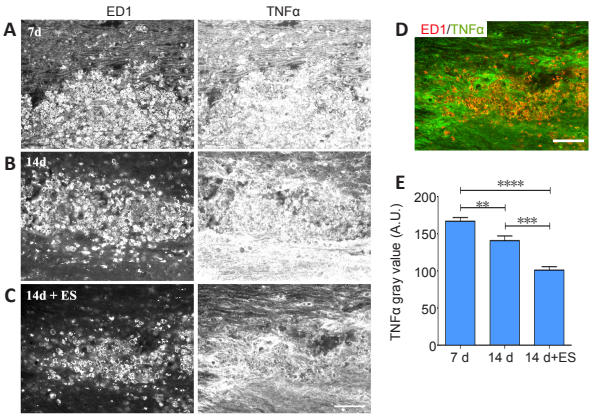

Figure 6 | Delayed brief ES diminishes levels of pro-inflammatory TNF-α protein in activated macrophages/microglia (ED-1) localizing to regions of focal DC demyelination.

(A–C) Longitudinal sections of dorsal spinal cord processed for dual immunofluorescence to detect activated microglia/macrophages (ED-1) and TNF-α. Prominent infiltration of TNF-α-/ED-1-positive immune cells into the demyelination zone occurs 7 days post-LPC/FG injection (A). One-hour ES at 7 days post-LPC diminishes the level of TNF-α detected at 14 days (C) relative to non-stimulated controls 14 days post-LPC (B). (D) Colocalization of the ED-1 and TNF-α images from the 14 days + ES time point in (C) where ED-1 is depicted as red and TNF-α as green shows that while the remaining macrophages/microglia express low levels of TNF-α (orange; D), the intense TNF-α expression does not localize in ED-1-positive cells (bright green regions; D). Note: the immune response (ED-1) appears to be more resolved in 14 days + ES tissue. Scale bar: 100 µm A–D. (E) Quantification of alterations in immunofluorescence signal intensity in focally demyelinated regions confirms qualitative observations. Data are expressed as the mean ± SEM. $n = 4$ animals analysed/experimental group. **$P < 0.01$, ****$P < 0.0001$ (one-way analysis of variance with Bonferroni's *post hoc* analysis).

Discussion

In the present study, we created a reproducible discrete unilateral focal demyelination of the DCs at the lumbar enlargement just above where sciatic nerve afferents enter, so that subsequent sciatic nerve ES would result in increased neural activity in this region. Examination of the effects that ES has on repair following focal DC demyelination revealed significant impacts on multiple repair indices beyond that previously described for myelination. These include increased expression of an axon-protective phenotype, enhanced presence/recruitment of oligodendrocytes/OPCs to the site of demyelination, increased linearized structures positive for MBP IF and paranodes as identified with the paranodal protein Caspr in the demyelination zones suggestive of increased myelination and polarization of activated macrophages/microglia in demyelination zones toward a pro-repair phenotype.

ES promotes an axon protective phenotype in focally demyelinated regions of DC

In this study, the presence of significantly more linear SMI-31/pNF-positive structures 7 days following the brief 1-hour ES implies that the axons present in the FG-intense demyelination zones are in a protected state. The phosphorylation state of the neuronal cytoskeletal protein neurofilament is an important indicator of whether the demyelinated axon is in a protected state. Dephosphorylated neurofilaments are susceptible to proteolysis by the calcium-dependent protease calpain (Greenwood et al., 1993), while phosphorylated neurofilaments are resistant to degradation (Pant, 1988). The addition of phosphate groups also increases the axonal caliber, an important determinant in the onset of myelination (Michailov et al., 2004).

ES enhances parameters associated with remyelination

The fact that significantly more Olig2-postive cells were observed in the focally demyelinated regions of the DC that underwent stimulation, indicates an increased presence of cells of the oligodendroglial lineage that can contribute to myelination. This significant difference in the number of Olig2-postive cells observed in the zone of demyelination in response to ES as compared to the 7- and 14-day post-LPC time points in the non-stimulated animals, suggests that ES may reduce expression of chemorepellent molecules such as Semaphorin-3A known to inhibit the infiltration of cells in the oligodendroglial lineage into zones of demyelination (Boyd et al., 2013), but this remains to be determined. Alternatively, it could be affecting the barrier set up by the mature oligodendrocytes bordering the lesion that tries to limit the demyelination (Macchi et al., 2020). Neuronal activity has been shown to regulate the differentiation of the OPC to a mature myelinating oligodendrocyte (Gautier et al., 2015; Gentile et al., 2019), once again emphasizing the importance of the axo-glial communication in driving myelination processes. Of note in the Gautier et al. (2015) study was the demonstration that demyelinated axons could still conduct actions potentials but do so in an impaired manner only at the speed of unmyelinated axons. Thus, the demyelinated axons in our present study can be depolarized by ES. Further, increased axonal activity drives the proliferation, differentiation and survival of myelinating glia (Demerens et al., 1996; Stevens et al., 1998; Gary et al., 2012; Gibson et al., 2014; Jensen and Yong, 2016; de Faria et al., 2019). Whether the increased numbers of Olig2-positive cells we observed in response to ES are due to increased recruitment and/or increased proliferation is unknown. But the enhanced OPC/oligodendrocyte presence and increased myelin profiles support that brief ES is having a positive impact on cellular constituents associated with remyelination, perhaps driving differentiation of OPC cells into oligodendrocytes. Even the lack of extensive myelin debris in the stimulated animals may be assisting in the response as it is necessary to drive the differentiation of OPCs into mature myelinating oligodendrocytes (Kotter et al., 2006; Neumann et al., 2009). The mechanism of how this increased axonal electrical activity improves remyelination was not investigated in the current study. However, Kukley et al. (2007) showed that activity-dependent axonal release of glutamate can serve as an instructive signal to oligodendrocytes to initiate cellular events associated with myelination *in vitro* (Wake et al., 2011) and more recently *in vivo* (Gibson et al., 2014; Gautier et al., 2015), Further, it has been recently shown that there is a preference for stimulated axons to be remyelinated (Mitew et al., 2018).

ES polarizes macrophages/microglia toward a pro-repair phenotype

Pro-inflammatory macrophages/microglia typically peak at onset of demyelinating disease and can be distinguished from pro-repair macrophages/microglia by their high levels of the pro-inflammatory cytokines, including TNF-α, interleukins IL-1β and IL-12 (Ambarus et al., 2012), as well as inducible nitric oxide synthase (Miron and Franklin, 2014). Pro-repair macrophages/microglia on the other hand, result from exposure of undifferentiated monocytes to molecules such as IL-4 or IL-10 leading to macrophages that secrete anti-inflammatory cytokines and neurotrophic factors and ones that effectively phagocytose myelin debris. Effectively ridding demyelinated areas of myelin debris is important as myelin inhibits OPC differentiation (Kotter et al., 2006). Pro-repair macrophages/microglia can be distinguished from pro-inflammatory macrophages/microglia by the expression of markers such as the mannose receptor CD206, Arg-1, CD163, transforming growth factor and IL-10.

By electrically stimulating sciatic nerve-derived DC axons we were able to switch the phenotype of macrophages/microglia from a proinflammatory phenotype toward a pro-repair phenotype consistent that described for macrophages in focally demyelinated peripheral nerve (McLean and Verge, 2016). The polarization state of macrophages/microglia can influence whether or not effective repair/remyelination will occur. High expression of pro-inflammatory relative to pro-repair molecules in these immune cells correlate with peak experimental autoimmune encephalomyelitis disease severity, while pro-repair macrophages/microglia are able to improve both oligodendrocyte differentiation and clinical presentation (Lloyd and Miron, 2016). Indeed the switch from a pro-inflammatory to a pro-repair phenotype correlates with the onset of myelination. Miron et al. (2013) showed both types of microglia contribute to OPC recruitment and proliferation, but only the pro-repair phenotype prevented OPC apoptosis and drove oligodendrocyte differentiation. Consistent with this are the elevated numbers of pro-repair polarized cells in post mortem MS tissue from active lesions relative to chronic lesions which do not remyelinate (Lloyd and Miron, 2016). Thus, it appears that therapies that increase neural activity hold the potential to favorably impinge on the pro-repair polarization axis and improve clinical outcomes. Collectively the ability of ES in the present study to polarize macrophages/microglia toward a pro-repair phenotype coupled with indicators of improved myelination support the validity of this strategy.

Potential limitations

While no single preclinical animal model of MS recapitulates all the aspects of MS pathogenesis, the LPC model has emerged as a strong model in which to study demyelination and remyelination events. This is primarily because the region

that is demyelinated can be precisely induced, in contrast to the more widely studied experimental autoimmune encephalomyelitis model of focal demyelination where the precise location of the lesions is not predictable (Lassmann and Bradl, 2017; Lamport et al., 2019). While LPC does effect a precise and robust focal demyelination in the injected area, a further challenge was ensuring that the LPC-demyelinated regions of dorsal columns contained sensory afferents from the sciatic nerve that was stimulated 7 days post LPC injection. Further, because the repair induced by the brief ES was so robust, it was also necessary to be able to identify the original area of the dorsal columns that was demyelinated by LPC. The novel inclusion of the retrograde tracer FG in the LPC injection cocktail served to both demarcate the region of focal demyelination (important when repair was robust) and retrogradely label the L4,5 DRG neurons. The latter assured that the region of the demyelinated dorsal columns being assessed contained sciatic nerve sensory afferents and thus had been effectively stimulated.

Conclusions

A 1-hour increase in axonal activity in focally demyelinated regions of the dorsal columns 7 days following a focal demyelinating lesion is sufficient to promote an axon protective phenotype, enhance the numbers of OPC/oligodendrocytes localizing to the demyelinated region and enhance myelination as detected by increased incidence of organized paranodes and linear MBP+ve structures observed. Coincident with these responses, stimulation also promoted a switch in phenotype of reactive macrophages/microglia from a pro-inflammatory toward a pro-repair state. These findings are in agreement with previously reported work in peripheral nerve focal demyelination model (McLean et al., 2014; McLean and Verge 2016). Thus, this study provides proof of principle for employment of strategies to increase axonal activity as a means to enhance repair and modulate the immune response following focal CNS demyelinating events.

Acknowledgments: *The authors would like to thank Ruiling Zhai (Department of Anatomy, Physiology and Pharmacology & CMSNRC, University of Saskatchewan) for her excellent technical assistance with the surgical procedures.*

Author contributions: *LA, NT, NAM, JMJ and VMKV participated in the conception, design, writing and interpretation of the research presented. LA, NAM conducted the surgeries; LA, NAM, NT and JMJ processed tissue for immunofluorescence and conducted image and data analysis. All authors approved the final version of the paper.*

Conflicts of interest: *The authors have no conflicts of interest to declare.*

Financial support: *This work was supported by Multiple Sclerosis Society of Canada (MSSOC), No. 2362 (to VMKV); Canadian Institutes of Health Research (CIHR), No. 14238 (to VMKV). LA and NT were supported by University of Saskatchewan College of Medicine Research Awards (CoMGRADs). The funders had no role in study design, data collection and analysis, decision to publish, or preparation of the manuscript.*

Institutional review board statement: *Animal care and experimental procedures were approved by the University of Saskatchewan's Animal Research Ethics Board (protocol# 20090087) on November 5, 2020.*

Copyright license agreement: *The Copyright License Agreement has been signed by all authors before publication.*

Data sharing statement: *Datasets analyzed during the current study are available from the corresponding author on reasonable request.*

Plagiarism check: *Checked twice by iThenticate.*

Peer review: *Externally peer reviewed.*

References

Ahn M, Lee C, Jung K, Kim H, Moon C, Sim KB, Shin T (2012) Immunohistochemical study of arginase-1 in the spinal cords of rats with clip compression injury. Brain Res 1445:11-19.

Al-Majed AA, Brushart TM, Gordon T (2000a) Electrical stimulation accelerates and increases expression of BDNF and trkB mRNA in regenerating rat femoral motoneurons. Eur J Neurosci 12:4381-4390.

Al-Majed AA, Neumann CM, Brushart TM, Gordon T (2000b) Brief electrical stimulation promotes the speed and accuracy of motor axonal regeneration. J Neurosci 20:2602-2608.

Ambarus CA, Krausz S, van Eijk M, Hamann J, Radstake TR, Reedquist KA, Tak PP, Baeten DL (2012) Systematic validation of specific phenotypic markers for in vitro polarized human macrophages. J Immunol Methods 375:196-206.

Banati RB, Gehrmann J, Schubert P, Kreutzberg GW (1993) Cytotoxicity of microglia. Glia 7:111-118.

Boyd A, Zhang H, Williams A (2013) Insufficient OPC migration into demyelinated lesions is a cause of poor remyelination in MS and mouse models. Acta Neuropathol 125:841-859.

Breder CD, Tsujimoto M, Terano Y, Scott DW, Saper CB (1993) Distribution and characterization of tumor necrosis factor-α-like immunoreactivity in the murine central nervous system. J Comp Neurol 337:543-567.

Cash E, Minty A, Ferrara P, Caput D, Fradelizi D, Rott O (1994) Macrophage-inactivating IL-13 suppresses experimental autoimmune encephalomyelitis in rats. J Immunol 153:4258-4267.

Chan JR, Watkins TA, Cosgaya JM, Zhang C, Chen L, Reichardt LF, Shooter EM, Barres BA (2004) NGF controls axonal receptivity to myelination by Schwann cells or oligodendrocytes. Neuron 43:183-191.

Choi S, Park C, Ahn M, Lee JH, Shin T (2012) Immunohistochemical study of arginase 1 and 2 in various tissues of rats. Acta Histochem 114:487-494.

Chung IY, Benveniste EN (1990) Tumor necrosis factor-α production by astrocytes. Induction by lipopolysaccharide, IFN-γ, and IL-1β . J Immunol 144:2999-3007.

Clerico M, Rivoiro C, Contessa G, Viglietti D, Durelli L (2008) The therapy of multiple sclerosis with immune-modulating or immunosuppressive drug. A critical evaluation based upon evidence based parameters and published systematic reviews. Clin Neurol Neurosurg 110:878-885.

David S, Kroner A (2011) Repertoire of microglial and macrophage responses after spinal cord injury. Nat Rev Neurosci 12:388-399.

de Faria O Jr, Gonsalvez DG, Nicholson M, Xiao J (2019) Activity-dependent central nervous system myelination throughout life. J Neurochem 148:447-461.

Demerens C, Stankoff B, Logak M, Anglade P, Allinquant B, Couraud F, Zalc B, Lubetzki C (1996) Induction of myelination in the central nervous system by electrical activity. Proc Natl Acad Sci U S A 93:9887-9892.

Faissner S, Plemel JR, Gold R, Yong VW (2019) Progressive multiple sclerosis: from pathophysiology to therapeutic strategies. Nat Rev Drug Discov 18:905-922.

Fitzgerald M (1987) Spontaneous and evoked activity of fetal primary afferents in vivio. Nature 326:603-605.

Fletcher JL, Murray SS, Xiao J (2018) Brain-derived neurotrophic factor in central nervous system myelination: a new mechanism to promote myelin plasticity and repair. Int J Mol Sci 19:4131.

Gahring LC, Carlson NG, Kulmar RA, Rogers SW (1996) Neuronal expression of tumor necrosis factor alpha in the murine brain. Neuroimmunomodulation 3:289-303.

Gary DS, Malone M, Capestany P, Houdayer T, McDonald JW (2012) Electrical stimulation promotes the survival of oligodendrocytes in mixed cortical cultures. J Neurosci Res 90:72-83.

Gautier HO, Evans KA, Volbracht K, James R, Sitnikov S, Lundgaard I, James F, Lao-Peregrin C, Reynolds R, Franklin RJ, Karadottir RT (2015) Neuronal activity regulates remyelination via glutamate signalling to oligodendrocyte progenitors. Nat Commun 6:8518.

Gentile A, Musella A, De Vito F, Rizzo FR, Fresegna D, Bullitta S, Vanni V, Guadalupi L, Stampanoni Bassi M, Buttari F, Centonze D, Mandolesi G (2019) Immunomodulatory effects of exercise in experimental multiple sclerosis. Front Immunol 10:2197.

Geremia NM, Gordon T, Brushart TM, Al-Majed AA, Verge VM (2007) Electrical stimulation promotes sensory neuron regeneration and growth-associated gene expression. Exp Neurol 205:347-359.

Gibson EM, Purger D, Mount CW, Goldstein AK, Lin GL, Wood LS, Inema I, Miller SE, Bieri G, Zuchero JB, Barres BA, Woo PJ, Vogel H, Monje M (2014) Neuronal activity promotes oligodendrogenesis and adaptive myelination in the mammalian brain. Science 344:1252304.

Goldstein ME, Sternberger NH, Sternberger LA (1987) Phosphorylation protects neurofilaments against proteolysis. J Neuroimmunol 14:149-160.

Gordon T, Udina E, Verge VM, de Chaves EI (2009) Brief electrical stimulation accelerates axon regeneration in the peripheral nervous system and promotes sensory axon regeneration in the central nervous system. Motor Control 13:412-441.

Greenwood JA, Troncoso JC, Costello AC, Johnson GV (1993) Phosphorylation modulates calpain-mediated proteolysis and calmodulin binding of the 200-kDa and 160-kDa neurofilament proteins. J Neurochem 61:191-199.

Ishibashi T, Dakin KA, Stevens B, Lee PR, Kozlov SV, Stewart CL, Fields RD (2006) Astrocytes promote myelination in response to electrical impulses. Neuron 49:823-832.

Jeffery ND, Blakemore WF (1995) Remyelination of mouse spinal cord axons demyelinated by local injection of lysolecithin. J Neurocytol 24:775-781.

Jensen SK, Yong VW (2016) Activity-dependent and experience-driven myelination provide new directions for the management of multiple sclerosis. Trends Neurosci 39:356-365.

Kataria H, Alizadeh A, Shahriary GM, Saboktakin Rizi S, Henrie R, Santhosh KT, Thliveris JA, Karimi-Abdolrezaee S (2018) Neuregulin-1 promotes remyelination and fosters a pro-regenerative inflammatory response in focal demyelinating lesions of the spinal cord. Glia 66:538-561.

Kotter MR, Zhao C, van Rooijen N, Franklin RJ (2005) Macrophage-depletion induced impairment of experimental CNS remyelination is associated with a reduced oligodendrocyte progenitor cell response and altered growth factor expression. Neurobiol Dis 18:166-175.

Kotter MR, Li WW, Zhao C, Franklin RJ (2006) Myelin impairs CNS remyelination by inhibiting oligodendrocyte precursor cell differentiation. J Neurosci 26:328-332.

Kukley M, Capetillo-Zarate E, Dietrich D (2007) Vesicular glutamate release from axons in white matter. Nat Neurosci 10:311-320.

Lamport AC, Chedrawe M, Nichols M, Robertson GS (2019) Experimental autoimmune encephalomyelitis accelerates remyelination after lysophosphatidylcholine-induced demyelination in the corpus callosum. J Neuroimmunol 334:576995.

Lassmann H, Bradl M (2017) Multiple sclerosis: experimental models and reality. Acta Neuropathol 133:223-244.

Lloyd AF, Miron VE (2016) Cellular and molecular mechanisms underpinning macrophage activation during remyelination. Front Cell Dev Biol 4:60.

Macchi M, Magalon K, Zimmer C, Peeva E, El Waly B, Brousse B, Jaekel S, Grobe K, Kiefer F, Williams A, Cayre M, Durbec P (2020) Mature oligodendrocytes bordering lesions limit demyelination and favor myelin repair via heparan sulfate production. Elife 9:e51735.

Mahad DH, Trapp BD, Lassmann H (2015) Pathological mechanisms in progressive multiple sclerosis. Lancet Neurol 14:183-193.

McLean NA, Verge VM (2016) Dynamic impact of brief electrical nerve stimulation on the neural immune axis-polarization of macrophages toward a pro-repair phenotype in demyelinated peripheral nerve. Glia 64:1546-1561.

McLean NA, Popescu BF, Gordon T, Zochodne DW, Verge VM (2014) Delayed nerve stimulation promotes axon-protective neurofilament phosphorylation, accelerates immune cell clearance and enhances remyelination in vivo in focally demyelinated nerves. PLoS One 9:e110174.

McTigue DM, Horner PJ, Stokes BT, Gage FH (1998) Neurotrophin-3 and brain-derived neurotrophic factor induce oligodendrocyte proliferation and myelination of regenerating axons in the contused adult rat spinal cord. J Neurosci 18:5354-5365.

Michailov GV, Sereda MW, Brinkmann BG, Fischer TM, Haug B, Birchmeier C, Role L, Lai C, Schwab MH, Nave KA (2004) Axonal neuregulin-1 regulates myelin sheath thickness. Science 304:700-703.

Miron VE, Franklin RJ (2014) Macrophages and CNS remyelination. J Neurochem 130:165-171.

Miron VE, Boyd A, Zhao JW, Yuen TJ, Ruckh JM, Shadrach JL, van Wijngaarden P, Wagers AJ, Williams A, Franklin RJM, Ffrench-Constant C (2013) M2 microglia and macrophages drive oligodendrocyte differentiation during CNS remyelination. Nat Neurosci 16:1211-1218.

Mitew S, Gobius I, Fenlon LR, McDougall SJ, Hawkes D, Xing YL, Bujalka H, Gundlach AL, Richards LJ, Kilpatrick TJ, Merson TD, Emery B (2018) Pharmacogenetic stimulation of neuronal activity increases myelination in an axon-specific manner. Nat Commun 9:306.

Monje M (2018) Myelin Plasticity and Nervous System Function. Annu Rev Neurosci 41:61-76.

Myers KJ, Dougherty JP, Ron Y (1993) In vivo antigen presentation by both brain parenchymal cells and hematopoietically derived cells during the induction of experimental autoimmune encephalomyelitis. J Immunol 151:2252-2260.

Nakahara J, Aiso S, Suzuki N (2009) Factors that retard remyelination in multiple sclerosis with a focus on TIP30: a novel therapeutic target. Expert Opin Ther Targets 13:1375-1386.

Neumann H, Kotter MR, Franklin RJM (2009) Debris clearance by microglia: an essential link between degeneration and regeneration. Brain 132:288-295.

Pant HC, Veeranna (1995) Neurofilament phosphorylation. Biochem Cell Biol 73:575-592.

Pant HC (1988) Dephosphorylation of neurofilament proteins enhances their susceptibility to degradation by calpain. Biochem J 256:665-668.

Prineas JW, Connell F (1979) Remyelination in multiple sclerosis. Ann Neurol 5:22-31.

Quirié A, Demougeot C, Bertrand N, Mossiat C, Garnier P, Marie C, Prigent-Tessier A (2013) Effect of stroke on arginase expression and localization in the rat brain. Eur J Neurosci 37:1193-1202.

Rawji KS, Yong VW (2013) The benefits and detriments of macrophages/microglia in models of multiple sclerosis. Clin Dev Immunol 2013:948976.

Singh S, Dallenga T, Winkler A, Roemer S, Maruschak B, Siebert H, Brück W, Stadelmann C (2017) Relationship of acute axonal damage, Wallerian degeneration, and clinical disability in multiple sclerosis. J Neuroinflammation 14:57.

Stevens B, Tanner S, Fields RD (1998) Control of myelination by specific patterns of neural impulses. J Neurosci 18:9303-9311.

Suminaite D, Lyons DA, Livesey MR (2019) Myelinated axon physiology and regulation of neural circuit function. Glia 67:2050-2062.

Tamatani M, Senba E, Tohyama M (1989) Calcitonin gene-related peptide- and substance P-containing primary afferent fibers in the dorsal column of the rat. Brain Res 495:122-130.

Tokuoka H, Saito T, Yorifuji H, Wei F, Kishimoto T, Hisanaga S (2000) Brain-derived neurotrophic factor-induced phosphorylation of neurofilament-H subunit in primary cultures of embryo rat cortical neurons. J Cell Sci 113(Pt 6):1059-1068.

Valério-Gomes B, Guimarães DM, Szczupak D, Lent R (2018) The absolute number of oligodendrocytes in the adult mouse brain. Front Neuroanat 12:90.

Wake H, Lee PR, Fields RD (2011) Control of local protein synthesis and initial events in myelination by action potentials. Science 333:1647-1651.

Zhang JY, Luo XG, Xian CJ, Liu ZH, Zhou XF (2000) Endogenous BDNF is required for myelination and regeneration of injured sciatic nerve in rodents. Eur J Neurosci 12:4171-4180.

C-Editors: Liu WJ, Li CH; T-Editor: Jia Y